J. exp. Biol. 151, 133–160 (1990)
Printed in Great Britain © *The Company of Biologists Limited 1990*

NONSPIKING PATHWAYS IN A JOINT-CONTROL LOOP OF THE STICK INSECT *CARAUSIUS MOROSUS*

BY ANSGAR BÜSCHGES*

Fachbereich Biologie, Universität Kaiserslautern, D-6750 Kaiserslautern, PB 3049, FRG

Accepted 15 February 1990

Summary

In the stick insect *Carausius morosus* (Phasmida) intracellular recordings were made from local nonspiking interneurones involved in the reflex activation of the extensor motoneurones of the femur–tibia joint during ramp-like stimulation of the transducer of this joint, the femoral chordotonal organ (ChO). The nonspiking interneurones in the femur–tibia control loop were characterized by their inputs from the ChO, their output properties onto the extensor motoneurones and their morphology. Eight different morphological and physiological types of nonspiking interneurones are described that are involved in the femur–tibia control loop. The results show that velocity signals from the ChO are the most important movement parameter processed by the nonspiking interneurones. Altering the membrane potential of these interneurones had marked effects on the reflex activation in the extensor motoneurones as the interneurones were able to increase or decrease the response of the participating motoneurones. The processing of information by the nonspiking pathways showed another remarkable aspect: nonspiking interneurones were found to process sensory information from the ChO onto extensor motoneurones in a way that seems not always to support the generation of the visible resistance reflexes in the extensor tibiae motoneurones in response to imposed flexion and extension movements of the joint. The present investigation demonstrated interneuronal pathways in the joint-control loop that show 'assisting' characteristics.

Introduction

In insects, investigation of the control of posture and the movement of single leg joints has led to extensive knowledge about the processing of sensory input that controls motor output in the thoracic nervous system (for reviews see Bässler, 1983*a*, 1988; Burrows, 1985, 1989; Burrows *et al.* 1988). However, the femur–tibia joint of the stick insect is the only insect leg joint that is well understood on the

* Present address: Department of Physiology, Faculty of Medicine, University of Alberta, Edmonton T6G 2H7, Canada.

Key words: stick insect, nonspiking interneurones, joint control, chordotonal organ, central processing.

basis of quantitative feedback loop analysis, although the neural basis of the control loop is unknown (Bässler 1983*a*, 1988). The position of this joint is measured by the femoral chordotonal organ (ChO). The ChO is separated from the muscles and so can be stimulated without any mechanical interference with the muscles or other sense organs. This has allowed the control system to be studied in the open-loop configuration with a mechanical input to the ChO and an output which can be measured as movement of the tibia or as muscle forces or as input or output of the motoneurones. The femur–tibia control system elicits different motor outputs in the active and inactive behavioural states of the stick insect (Bässler, 1988). In the present study the femur–tibia control loop has been investigated in the *inactive* animal. In this situation, imposed movements of the tibia or equivalent movements of the ChO induce resistance reflexes in both antagonistic muscles of the joint, the flexor and extensor tibiae.

The study of the neural basis of the femur–tibia control system started with an investigation of the receptor cells of the ChO. It was found that they measure the position, the velocity or the acceleration of the tibia, either alone or in various combinations (Hofmann *et al.* 1985; Hofmann and Koch, 1985). These findings explain the velocity- and position-sensitivity of the system (Bässler, 1983*a*).

The pathways between the ChO and the motoneurones of the flexor and the extensor muscles in the stick insect that generate the resistance reflex in the inactive animal are unknown. In the locust metathorax, different pathways from the ChO to these motoneurones have been described (Laurent and Burrows, 1988; Burrows *et al.* 1988). The significance of these pathways for the characteristics of the whole system remains unclear. It is probable that in the stick insect there are comparable pathways, with monosynaptic connections, connections *via* nonspiking interneurones, connections *via* spiking interneurones and connections with different intercalated interneurones between the ChO and the motoneurones. This will be verified for nonspiking interneurones in this paper.

The output side of the femur–tibia control loop consists of two parts, the extensor tibiae and the flexor tibiae muscles with their motoneurones. The membrane potentials of the two excitatory extensor motoneurones, the slow extensor tibiae (SETi) and the fast extensor tibiae (FETi), are influenced in the same way by a given stimulus to the ChO (Bässler, 1983*b*; Kittmann, 1984). The flexor part of the control loop is more complex (Debrodt and Bässler, 1989, 1990). The membrane potentials of the different excitatory motoneurones of the flexor muscle can differ from one another for the same stimulus to the ChO (Debrodt and Bässler, 1989, 1990).

The present paper investigates the role of nonspiking interneurones in the extensor part of the femur–tibia control loop in the inactive animal (see also Bässler, 1988; Büschges, 1989*b*). The extensor part of the control loop was chosen because it contains only two excitatory motoneurones that can be monitored rather simply by extracellular recording from the extensor nerve F2. The slow extensor tibiae motoneurone (SETi) is also spontaneously active. By comparison, the innervation of the flexor muscle is more complex, does not offer the possibility

of easy and complete output monitoring, and the motoneurones are normally not spontaneously active (Debrodt and Bässler, 1989, 1990).

Materials and methods

All experiments were performed on adult female *Carausius morosus* from our colony at the University of Kaiserslautern. The animals were mounted dorsal-side-up on a platform. The middle legs and the meso- and metathoracic segments were placed inside an enclosure (20 mm×60 mm) filled with *Carausius* saline (Weidler and Diecke, 1969; Bässler, 1977). The left middle leg was fixed perpendicular to the thorax, in such a way that the femur–tibia joint angle was a right angle and the tibia pointed down. A small opening was made in the femur and the receptor apodeme of the ChO was fixed in a clamp and cut distal to the clamp (for details of stimulation procedure, see Büschges, 1989*a*; Hofmann and Koch, 1985). Ramp-and-hold displacement stimuli of 100 μm amplitude were applied to the ChO. The reference point of the stimulation was the 90° position of the joint. A displacement of the ChO by 100 μm corresponds to a joint movement of about 20° in *Carausius* (Weiland *et al.* 1986). The values of the movement parameters are given in mm, $mm\,s^{-1}$ or $mm\,s^{-2}$. As an aid to understanding, angular units describing the mimicked movements of the femur–tibia joint (degrees, $degrees\,s^{-1}$, $degrees\,s^{-2}$) are sometimes appended in parentheses (for an explanation see Büschges, 1989*a*). In the same way 'flexion' and 'extension' are sometimes used to explain the stimulus to the ChO. The velocities of the different ramp-and-hold stimuli ranged from 0.05 to $27.8\,mm\,s^{-1}$ (approx. $10–5.56\times10^{3}\,degrees\,s^{-1}$), and acceleration ranged from 0.3 to $39\,700\,mm\,s^{-2}$ (approx. $60–7.94\times10^{6}\,degrees\,s^{-2}$). To investigate the effects of ChO position, ChO positions of −100 μm (approx. 110°), 0 μm (approx. 90°), +100 μm (approx. 70°) and +200 μm (approx. 50°) were tested (for a definition of position, velocity and acceleration signs, see Büschges, 1989*a*) and a change in the membrane potential was measured relative to the membrane potential at the reference point (90°). The tested parameter values are within the range of values used in previous investigations of the femur–tibia control loop of the stick insect (for details see Bässler, 1983*a*; Hofmann *et al.* 1985; Hofmann and Koch, 1985). The physiology of the chordotonal organ sensory cells has been described (Hofmann *et al.* 1985; Hofmann and Koch, 1985), and it has been shown that the sensory cells in the chordotonal organ are able to distinguish accurately between position, velocity and acceleration signals of movements of the receptor apodeme.

The activity of the extensor tibiae motoneurones was recorded by using an extracellular hook electrode (Schmitz *et al.* 1988) attached to nerve F2 in the femur. For intracellular recordings, the body of the stick insect was opened from the dorsal side. The gut and fat tissue were removed and the mesothoracic ganglion was lifted onto a wax-coated platform and fixed with small cactus spines. The recording and staining procedures were as described by Büschges (1989*a*).

Recordings of the nonspiking interneurones, together with position and velocity

signals of the stimuli, extracellular nerve (F2) recordings, current monitor and stimulus trigger signals were stored on magnetic tape (Racal Store 7DS) for later display and evaluation on a Transient recorder (Physirec by L. Neumann) or on a Gould ES 1000 chart recorder. Signal averaging (shown for example in Fig. 5C) was performed by using an A/D converter (IBM data acquisition and control adapter), a computer (IBM AT-02) and a special averaging program (written by A. Ruppel, 1988). An amplitude and peak window discriminator (designed by P. Heinecke after Zarnack and Möhl, 1976) was used to convert spikes to TTL signals (0–5 V square-wave signals). Peristimulus time histograms were generated using an Apple IIe microcomputer with a special interface (designed by M. Spüler).

Results

Recordings were made in the dorsal neuropile of the mesothoracic ganglion ipsilateral to the stimulated ChO, an area comparable to that chosen by Siegler and Burrows (1979) (see Fig. 1). Recordings were made from nonspiking interneurones that had the following characteristics: (1) ChO signals of elongation or relaxation movements induced reproducible responses in the interneurone; (2) changing the membrane potential of the recorded interneurone by current injection modulated the activity of one or both excitatory extensor motoneurones (FETi and SETi). Depolarization of all the recorded interneurones markedly altered SETi activity (increasing or decreasing the discharge rate).

Neurones were considered to be nonspiking if, during the whole recording, no spike occurred, and if the following six criteria [see also Burrows (1981), Siegler (1985), Wilson (1981) and Hengstenberg (1977)] were fulfilled: (a) all stimuli applied to the ChO failed to induce spike generation; (b) unspecific tactile stimulation did not cause spikes; (c) spikes were not generated during a change in the behavioural state of the animal (Bässler, 1988; Büschges, 1989*b*); (d) there was no spike generation after a long and large hyperpolarization; (e) depolarization of these interneurones changed the amplitude of EPSPs without inducing spikes; and (f) graded effects on the activity of postsynaptic motoneurones were recorded without the occurrence of spikes in the interneurone.

Altogether recordings were made from more than 70 nonspiking interneurones of which 25 fulfilled criteria 1 and 2 (see above). These were classified according to the influence of an artificial depolarization on the extensor motoneurones (E, excitatory; I, inhibitory) and according to morphological and physiological characteristics. The morphological classification of the neurones was based on the characteristics of the gross morphology of the neurones: soma location, primary neurite and arborization pattern, as seen in whole-mounts.

Latency is defined as the time between the beginning of the acceleration of the stimulus and the beginning of a change in membrane potential of the recorded interneurone. As it is obvious that the parameter values of the applied stimuli influence the measured latencies (see Büschges, 1989*a*), the latencies were

obtained using 'faster' stimuli. The parameter values of the stimuli used are always given.

Nonspiking interneurones with excitatory effects on the activity of the extensor motoneurones

Six distinct morphological types of interneurones were found which, when depolarized by current injection, increased the spike frequency of one or both extensor motoneurones, SETi or FETi. All neurones were depolarized by elongation stimuli (joint flexion).

Type E1 (number of recordings: N=*1)*

The first type of interneurone was depolarized only during elongation (joint flexion) of the ChO. It influenced SETi as well as FETi. The soma of this type of interneurone lay ventrally in the posterior ipsilateral part (ipsilateral to the stimulated ChO) of the ganglion. The arborizations were mainly dorsally located (Fig. 1).

Elongation stimuli induced a marked depolarization in response to stimuli with a velocity less than $+0.3\,\mathrm{mm\,s^{-1}}$ ($+60\,\mathrm{degrees\,s^{-1}}$). At a stimulus velocity of $+0.98\,\mathrm{mm\,s^{-1}}$ ($+200\,\mathrm{degrees\,s^{-1}}$) and an acceleration of $\pm 300\,\mathrm{mm\,s^{-2}}$ ($\pm 6\times 10^4\,\mathrm{degrees\,s^{-2}}$) the depolarization started in this interneurone after a mean

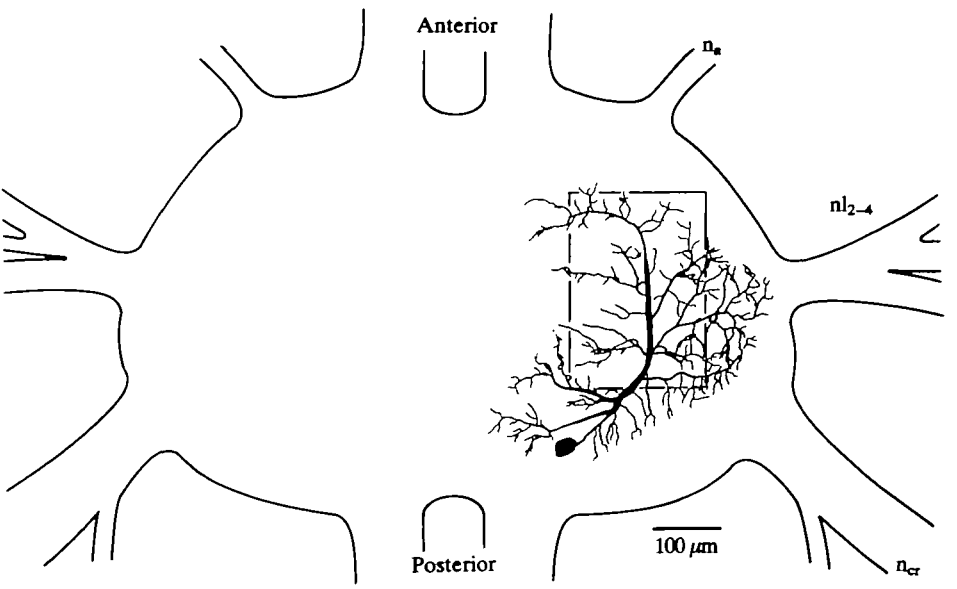

Fig. 1. Morphology of a nonspiking interneurone in the mesothoracic ganglion of *Carausius morosus* transmitting sensory information from the chordotonal organ (ChO) onto the excitatory extensor motoneurones. View from the ventral side. The stimulated ChO is located on the right side of the drawing. The marked area shows the recording region in the ganglion. n_a, nervus anterior; nl_{2-4}, nervus lateralis 2–4; n_{cr}, nervus cruris.

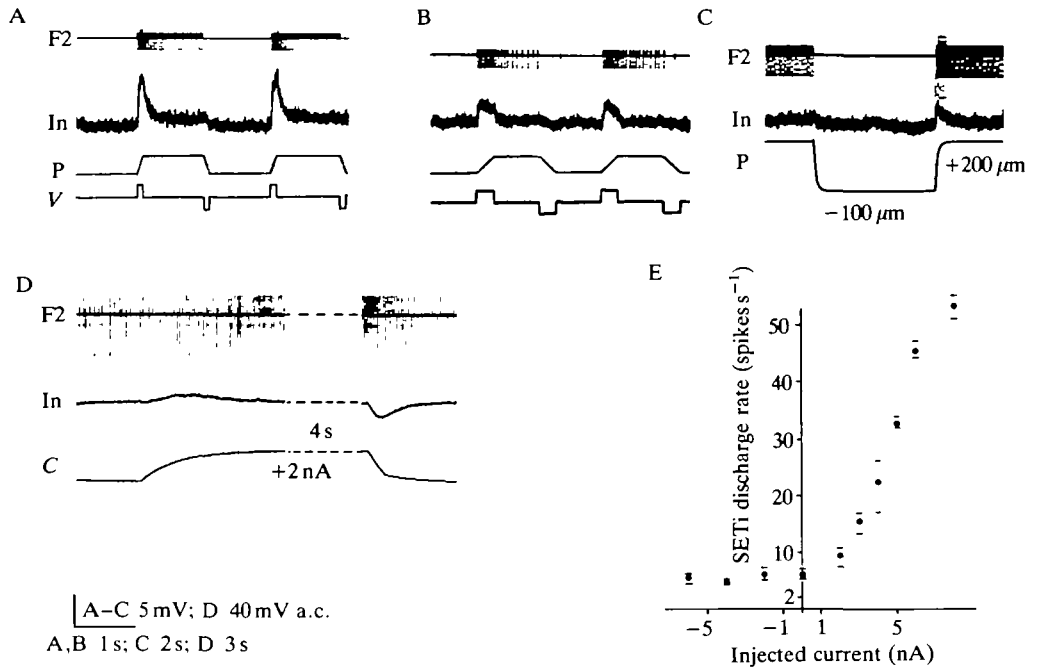

Fig. 2. Physiological properties of the interneurone shown in Fig. 1. (A,B) Ramp-and-hold stimulation of the ChO; (C) test of tonic position effects by the ChO afferences on the membrane potential of the recorded interneurone (−100 μm, approx. 110°; +200 μm, approx. 50°); (D) effects of depolarization of the interneurone on the SETi activity; (E) relationship between the current injected into the interneurone and the SETi discharge rate measured at the 90° position of the ChO (mean SETi activity over 6 s, minimum and maximum values are shown). F2, extensor nerve; In, interneurone; P, position of the ChO; *V*, velocity; *C*, current.

latency of 7.2±1.9 ms (mean±S.D., $N=10$, where N is the number of averaged events). The amplitude of depolarization during elongation ramps was greater for fast stimuli than for slow ones (Fig. 2A,B). In the elongated position (Fig. 2A,B) the membrane potential was slightly reduced. However, the membrane potential did not systematically depend on the ChO position, tested over a broader range between −100 μm (approx. 110°) and +200 μm (approx. 50°) (Fig. 2C). Relaxation of the ChO produced no measurable effects (Fig. 2A–C). As single IPSPs were visible during the recording of the interneurone, the possibility that the interneurone was hyperpolarized during relaxation stimuli at the ChO can probably be excluded.

Changing the membrane potential of this interneurone by injecting depolarizing currents caused an increase of spike frequency in the SETi motoneurone (Fig. 2D,E). Hyperpolarizing currents had no effect on the SETi discharge rate (Fig. 2E). Applying depolarizing currents greater than +5 nA also induced

activity of the FETi motoneurone after some seconds. The effect of applying depolarizing currents during ChO stimulation (see type E2) was not tested.

The results show that this neurone (like types E2 and E3) transmits sensory information from the ChO to the excitatory extensor motoneurones and that it is therefore involved in the mediation of the resistance reflex in the extensor motoneurones during elongation stimuli (joint flexion) at the ChO (see also Fig. 17, Ib).

Type E2 (N=1)

The reactions of the second type of interneurone, whose morphology is shown in Fig. 3A, were comparable to those of type E1 (see also Fig. 17, Ib). The soma of this type lay laterally in the posterior part of the ganglion on a level with the entrance of the posterior connectives. The arborizations were mainly located dorsally.

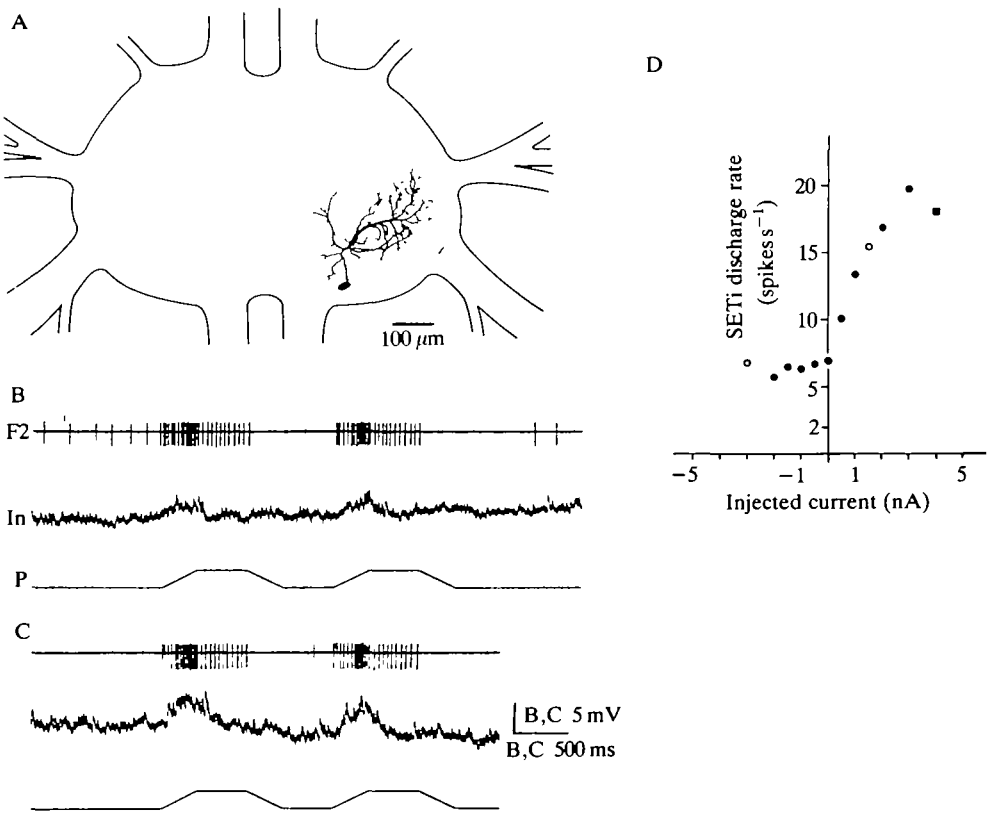

Fig. 3. Morphological and physiological properties of a nonspiking interneurone in the femur–tibia control loop. (A) Morphology; (B) interneuronal response to ramp-and-hold stimulation of the ChO; (C) the same experiment as in B but the interneurone is slightly hyperpolarized (−1 nA); (D) plot of mean SETi discharge rate against current injected into the interneurone (● 7 s, ○ 5 s, ■ 2 s). F2, extensor nerve; In, interneurone; P, position.

Elongation stimuli (joint flexion) caused a depolarization during the ramp phase of the stimulus without a tonic component (Fig. 3B,C). The mean latency between stimulus onset and depolarization was 10.1±6.6 ms [N=11, velocity=+0.3 mm s^{-1} (approx. +60 degrees s^{-1}), acceleration=±10.3 mm s^{-2} (approx. ±2×10^3 degrees s^{-2})]. The amplitude of depolarization increased with stimulus velocity. Relaxation stimuli (joint extension) produced no measurable reactions (depolarizing the interneurone by current injection during relaxation ramps showed no enlarged IPSPs, which might have passed unnoticed at the resting potential of the interneurone).

Depolarizing the interneurone by current injection caused an increase of the SETi discharge rate from 7 spikes s^{-1} (0 nA) to a frequency of about 20 spikes s^{-1} (+3 nA). Hyperpolarizing currents did not affect the SETi discharge rate (Fig. 3D). There was no detectable effect on FETi activity. Changing the membrane potential of this interneurone tonically by injection of depolarizing currents during and after elongation stimuli caused an increase in the reflex activation of the SETi (Fig. 4A–D). Hyperpolarizing the interneurone had no detectable effect on SETi activity during the resistance reflex.

Type E3 (N=4)

The third type of interneurone had a slight tonic component. Its morphology is shown in Fig. 5A,B. The soma lay ventrally towards the posterior part of the

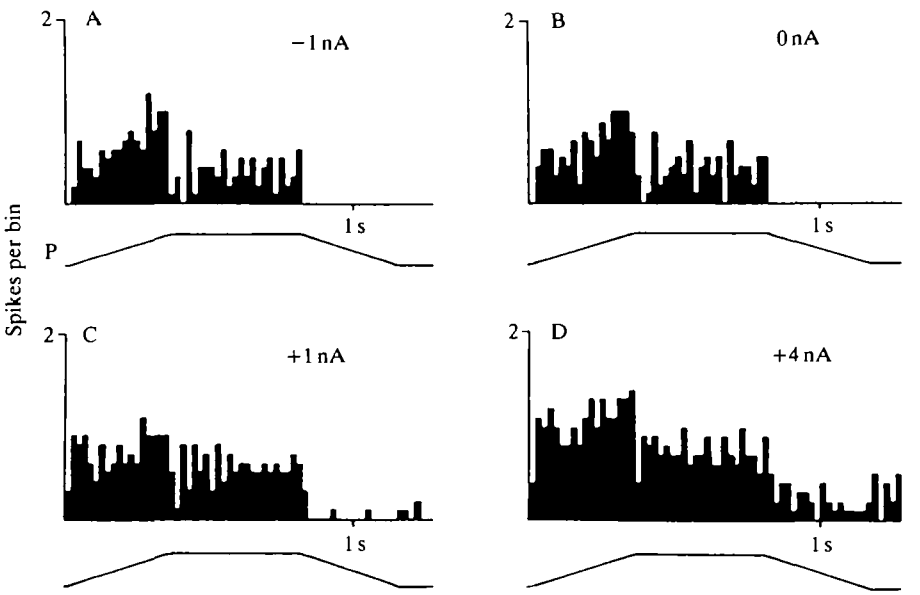

Fig. 4. Modulation of the resistance reflex in the SETi motoneurone during ChO stimulation by injection of current into the nonspiking interneurone shown in Fig. 3. Each peristimulus time histogram represents an average of 10 events with the following mean SETi activities: (A) 19.1 spikes $stimulus^{-1}$; (B) 19.5 spikes $stimulus^{-1}$; (C) 26.7 spikes $stimulus^{-1}$; (D) 41.5 spikes $stimulus^{-1}$.

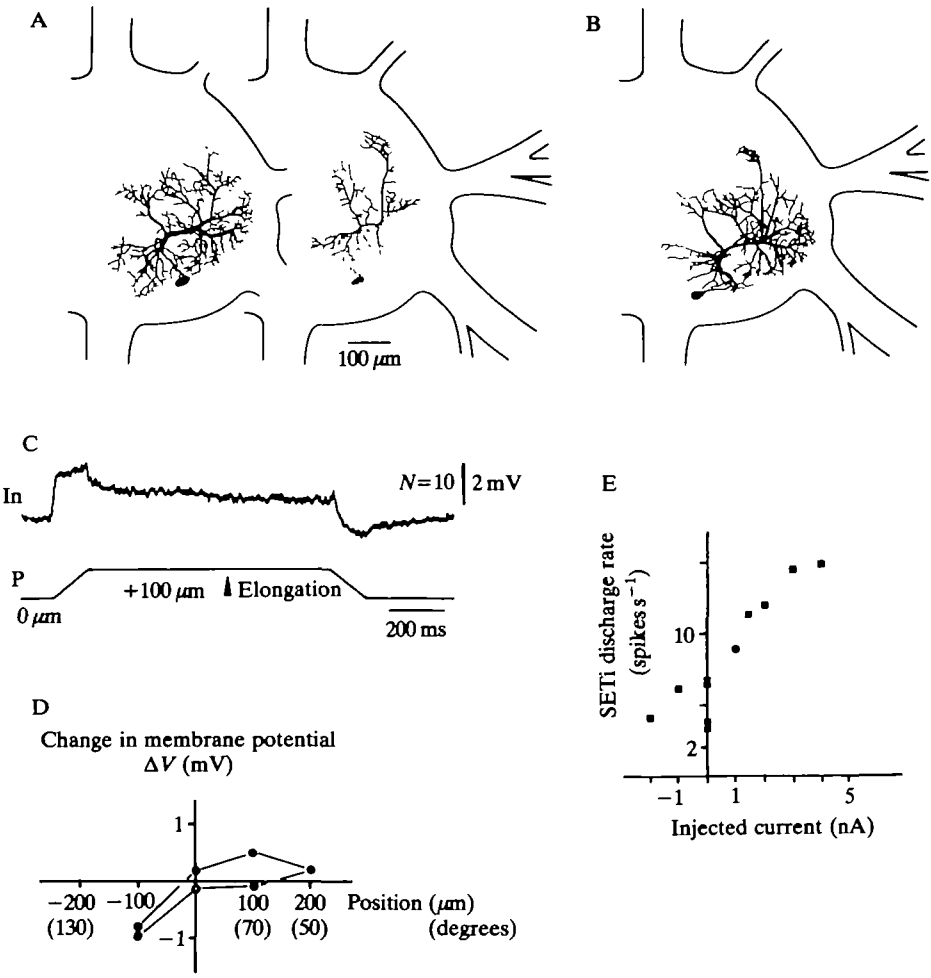

Fig. 5. Morphological and physiological properties of interneurones of type E3. (A,B) Morphology of two nonspiking interneurones of this type; (C) response of the interneurone shown in A to ramp-and-hold stimuli at the ChO, shown in the form of an average over 10 ramp-and-hold stimuli; (D) plot of the change in membrane potential of the interneurone shown in A *versus* ChO positions measured 4 s after every change of ChO position [measured from the starting position at −100 μm (approx. 110°) to +200 μm (●) and back to −100 μm (○)]; (E) relationship between the current injected into the interneurone and the mean SETi discharge rate (■ 6 s, ● 4 s).

ganglion. The arborizations of this type of interneurone were primarily median and dorsally located. One prominent branch (see Fig. 5A,B) ran directly towards the entrance of the nervus anterior and ended in the most anterior position of all the arborizations (Fig. 5A,B).

Elongation ramps at the ChO with a stimulus velocity of less than +0.3 mm s^{-1} (approx. 60 degrees s^{-1}) induced a depolarization that outlasted the stimulus ramp (see Fig. 17, Ia). The amplitude of depolarization during the position transient of

the ramp-and-hold stimulus increased with increasing stimulus velocities. The mean latency was 5.2±0.4 ms (N=5) for elongation stimuli [velocity= +1.0 mm s^{-1} (approx. +200 degrees s^{-2}), acceleration=±147.9 mm s^{-2} (approx. ±3.0×10^4 degrees s^{-2})]. Besides these physiological similarities to types E1 and E2 neurones, the membrane potential of type E3 interneurones showed a slight tonic dependence on the position of the ChO (Fig. 5C,D). More elongated positions of the ChO were coupled to a slightly more depolarized membrane potential in this interneurone (Fig. 5D) measured between −100 μm (110°) and +200 μm (50°).

Relaxation stimuli induced a hyperpolarization in this interneurone (Fig. 5C). In some cases, fast stimuli [velocity=±9.3 mm s^{-1} (approx. ±1860 degrees s^{-1}), acceleration=±0.68 m s^{-2} (approx. ±1.4×10^4 degrees s^{-2})] induced small depolarizations with a latency of more than 10 ms, but this did not always occur.

Depolarizing currents injected into interneurones of this type increased tonic SETi activity. This effect also persisted during stimulation of the ChO (comparable to Fig. 4). In no recording was FETi activity influenced.

Type E4 (N=*11*)

The following three types (E4–E6) of nonspiking neurones were depolarized not only by elongation stimuli (corresponding to joint flexion) but also by relaxation stimuli. Fig. 6A,B shows two interneurones of the morphological type E4. Their morphology closely resembled a morphological type of nonspiking interneurone described by other authors in the meso- and metathoracic ganglia of the locust (Siegler and Burrows, 1979; Wilson, 1981; Watkins *et al.* 1985). The soma lay ventrally, contralateral to the stimulated ChO. The primary neurite crossed the midline and arborized mainly dorsally and ipsilaterally to the stimulated ChO.

The neurone shown in Fig. 6A depolarized (summed and single EPSPs) in response to elongation stimuli (joint flexion) with positive stimulus velocities of +0.3 mm s^{-1} (approx. +60 degrees s^{-1}) or greater (Fig. 7). Relaxation stimuli, which give negative velocities (joint extension), induced a detectable response to stimulus velocities of −1.0 mm s^{-1} (approx. −200 degrees s^{-1}) or greater (Fig. 7). In the elongation direction [tested for stimuli with velocity=+9.4 mm s^{-1} (approx. +1860 degrees s^{-1}); acceleration=±1.4 m s^{-2} (approx. ±2.8×10^5 degrees s^{-2})] the depolarization occurred with a constant mean latency of 5 ms (N=5); in the relaxation direction the mean latency was 5.4±0.5 ms (N=5). For all other recordings of interneurones of this type the measured latencies were constant for each animal and varied from animal to animal from 4 to 6 ms both for elongation and for relaxation stimuli. In all recordings the amplitude of depolarization was greater for elongation (joint flexion) than for relaxation stimuli (joint extension). The depolarization increased with increasing stimulus velocity and was not position-dependent. Applying stimuli with a constant maximum velocity but with varying acceleration (Fig. 8A–C) showed that the amplitude of depolarization depended mainly on the stimulus velocity (see also Fig. 8D for the interneurone

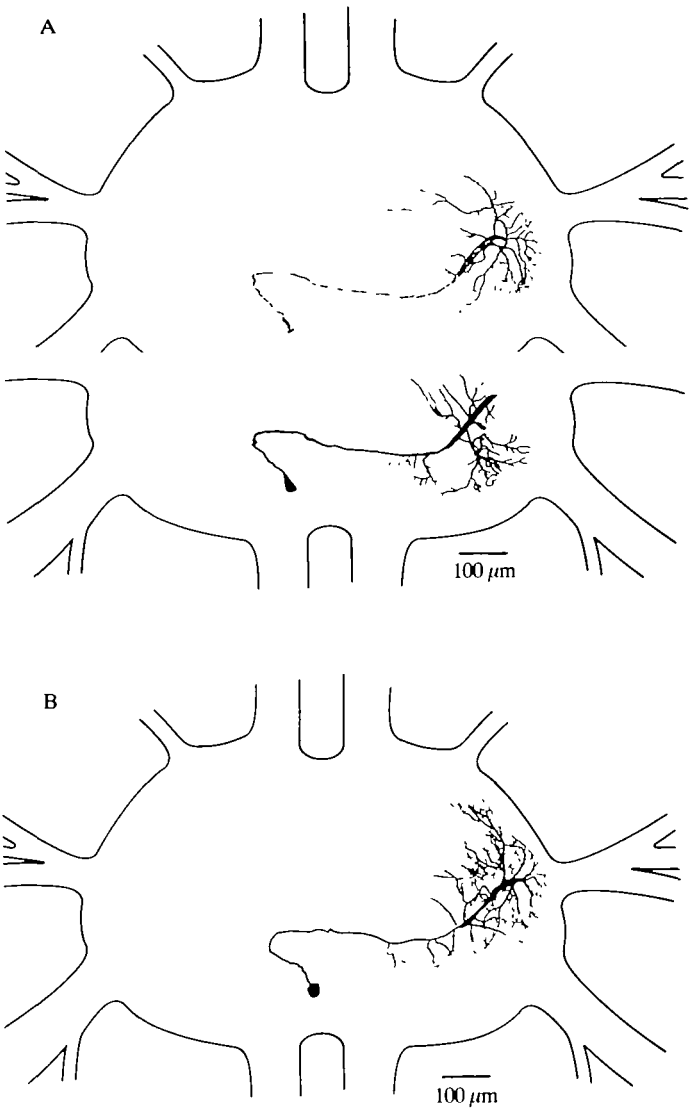

Fig. 6. (A,B) Two interneurones with a very similar morphology and physiology (type E4). In A, dorsal arborizations (upper part) are drawn separate from median and ventral arborizations (lower part).

shown in Fig. 6A). This was true for elongation as well as for relaxation stimuli. Acceleration had only a slight influence on the depolarization amplitude (Fig. 8E). (The fact that the stimulus amplitude was fixed may mean that the attainment of higher stimulus velocities requires higher acceleration. This might mimic an influence of acceleration on the response in the interneurone.)

Injection of depolarizing currents (Fig. 9) increased the SETi discharge rate. In four cases larger depolarization of the interneurones also induced FETi spikes.

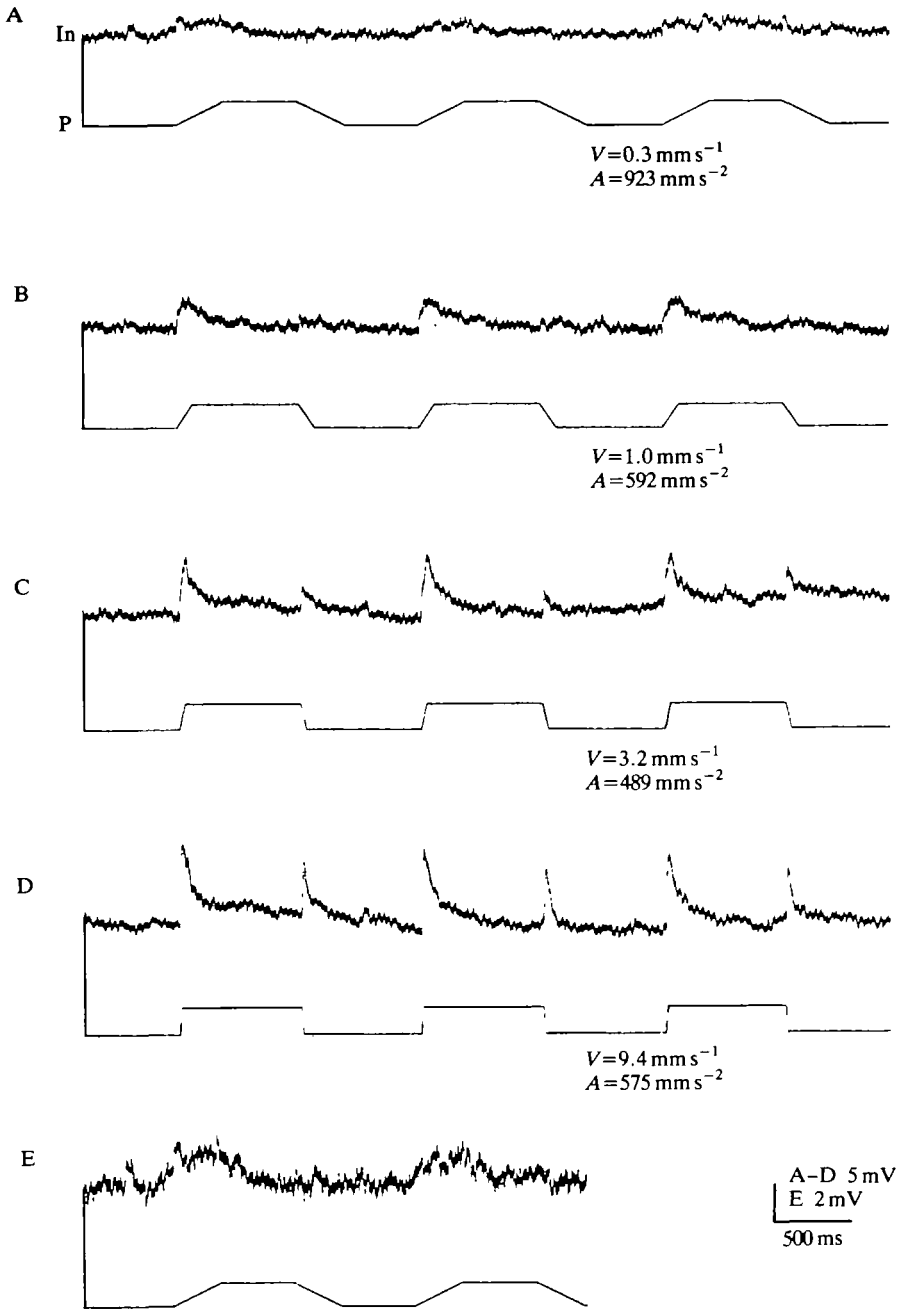

Fig. 7. Physiology of the interneurone shown in Fig. 6A. Response of the interneurone to varying stimuli to the ChO (A–D). In E the interneuronal response in A is shown on an enlarged scale. Angular units of the mimicked movement: (A) velocity=± 60 degrees s^{-1}, acceleration=$\pm 1.8\times 10^5$ degrees s^{-2}; (B) velocity=± 200 degrees s^{-1}, acceleration=$\pm 1.2\times 10^5$ degrees s^{-2}; (C) velocity=± 640 degrees s^{-1}, acceleration=$\pm 9.8\times 10^4$ degrees s^{-2}; (D) velocity=$\pm 1.9\times 10^3$ degrees s^{-1}, acceleration=$\pm 1.2\times 10^5$ degrees s^{-2}; (E) as in A.

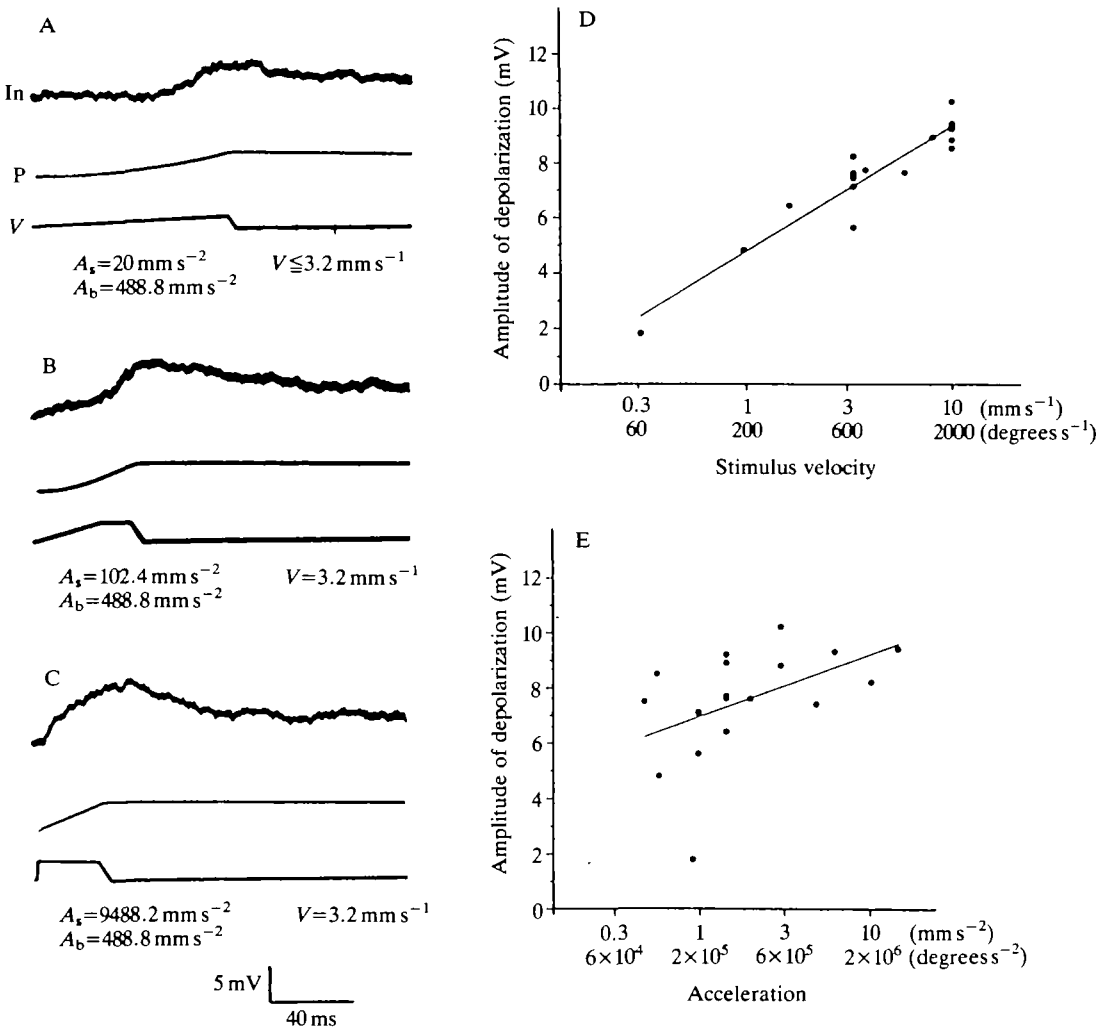

Fig. 8. Analysis of the response of the interneurone shown in Fig. 6A to elongation stimuli at the ChO. (A–C) Changes of membrane potential of the interneurone during different elongation ramps with the same velocity, but different starting accelerations. Angular units of the mimicked movement: (A–C) velocity=+640 degrees s^{-1}, A_b (see below)=−9.8×10^4 degrees s^{-2}; (A) A_s (see below)=+4×10^3 degrees s^{-2}; (B) A_s=+2×10^4 degrees s^{-2}; (C) A_s=1.9×10^6 degrees s^{-2}). (D,E) Plot of the mean depolarization (N=5) of the interneurone during elongation ramps *versus* stimulus velocity (D, regression coefficient=0.95) and stimulus acceleration (E, regression coefficient=0.48). In, interneurone; P, position; V, velocity; A_s, acceleration of the starting phase of the ramp; A_b, acceleration of the braking phase of the ramp.

Injecting hyperpolarizing currents into the interneurone did not influence SETi activity. Depolarizing this type of interneurone while stimulating the ChO increased SETi activity during reflex activation. Although SETi activity was still inhibited during relaxation ramps, single SETi spikes were detectable during the

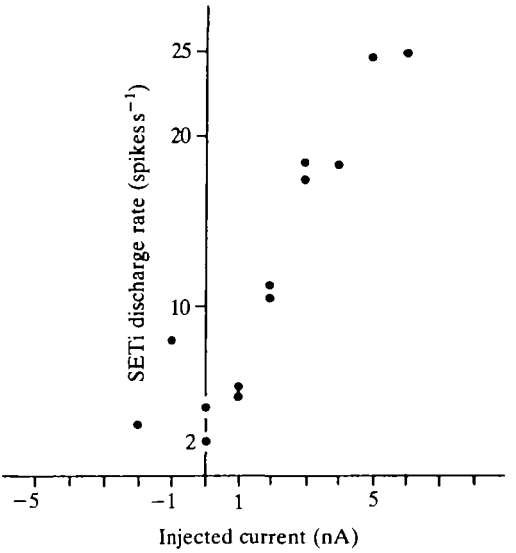

Fig. 9. Relationship between the current injected into the interneurone shown in Fig. 6A and the mean SETi discharge rate (averaged over 4 s).

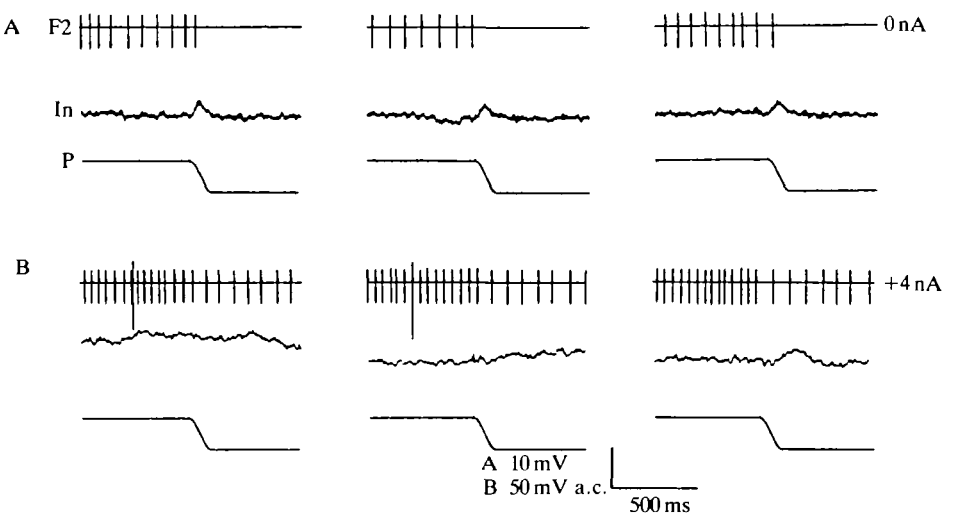

Fig. 10. Depolarization of interneurones of type E4 causes SETi spikes to occur during relaxation ramps of the ChO (see text). (A) Relaxation ramps at the resting potential of the interneurone; (B) relaxation ramps during depolarization of the interneurone. F2, extensor nerve; In, interneurone; P, position.

relaxation phase of the trapezoidal stimuli (Fig. 10; normally relaxation of the ChO with this type of stimulus inactivates the SETi motoneurone totally).

Thus, this type of interneurone is involved in the generation of the resistance

reflex in the extensor motoneurone during elongation stimuli. However, the physiological properties of these interneurones are obviously complex, as they were also depolarized by ChO signals during relaxation stimuli (see Fig. 17, IIa, and Discussion).

Type E5 (N=2)

The soma of the fifth morphological type of interneurone lay anterior to the point of entry of nerves nl_{2-4} on the ventral side of the ganglion (Fig. 11A). The main arborizations were located in the median and dorsal part of the ganglion.

Elongation and relaxation ramps induced a depolarization in these interneurones similar to that of the type E4 interneurones. Depolarization was caused by stimuli with a velocity lower than $\pm 0.3\,mm\,s^{-1}$ (± 60 degrees s^{-1}). The latencies were 5 ms ($N=5$) for elongation ramps and 5.6 ms for relaxation ramps [with velocity $=\pm 3.2\,mm\,s^{-1}$ (approx. ± 640 degrees s^{-1}), acceleration $=\pm 488.8\,mm\,s^{-2}$ (approx. $\pm 9.8\times 10^4$ degrees s^{-2})] (Fig. 11B).

Depolarizations caused by relaxation ramps were always greater in amplitude than those caused by elongation ramps (Fig. 11B). The amplitude of depolarization increased with faster stimuli. From the data it is not clear whether the depolarization was induced by stimulus velocity or by stimulus acceleration. The response duration in the interneurone during slow stimuli (where the response outlasts the whole stimulus) suggests that it is stimulus velocity that caused the response in the interneurone. In some cases small single depolarizations (EPSPs) or hyperpolarizations (IPSPs) were visible at the end of fast elongation and relaxation stimuli, but their occurrence could not be shown to be a repeatable effect of the stimulus. There was no detectable tonic position component on the membrane potential.

Depolarizing the interneurones by current injection (in Fig. 11C,D) increased the mean activity of the SETi motoneurone (0 nA: 0.5 Hz; +2 nA: 19.6 Hz, averaged over 8 s). Hyperpolarizing currents had no effect on the SETi discharge rate. The FETi motoneurone was not affected by injection of current into the interneurone. Injecting depolarizing current during ramp-and-hold stimulation of the ChO caused an increase of SETi activity during the static (elongated or relaxed) and the dynamic (elongation and relaxation) phases of the stimulus (Fig. 11C, see also Fig. 17, IIa).

Type E6

One interneurone was found that was rather strongly tonically affected by ChO position (Fig. 12). The gross morphology and the response characteristics during position transients at the ChO were similar to those of interneurones of type E5 (Fig. 11, see also Fig. 17, IIa). As has been shown for interneurones of types E2–E5, this interneurone influenced the activity of the SETi motoneurone when the ChO position was static, as well as during elongation and relaxation movements at the ChO. Despite the morphological and physiological similarities to the interneurones of type E5, the remarkable position-dependence of the

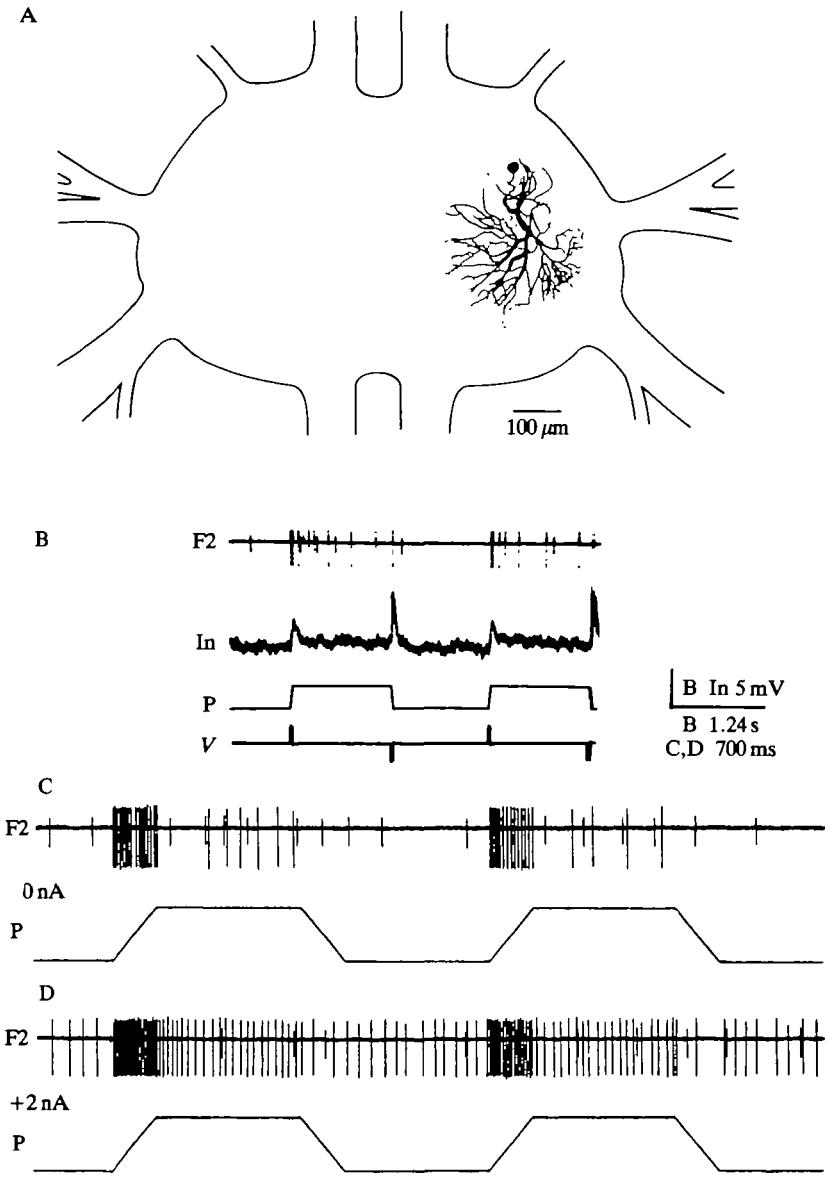

Fig. 11. Morphological and physiological properties of a nonspiking interneurone of type E5. (A) Morphology; (B) recording of the membrane potential of the interneurone during trapezoidal stimulation of the ChO; (C,D) SETi activity during trapezoidal stimuli of the ChO when different currents were injected into the interneurone. F2, extensor nerve; In, interneurone; P, position; *V*, velocity.

membrane potential of this interneurone led to its classification in a separate category (Fig. 12B). Over a range of 300 μm (50–110°) the membrane potential depended on ChO position and increased with more elongated positions. Possible hysteresis effects were not investigated in detail (Fig. 12B).

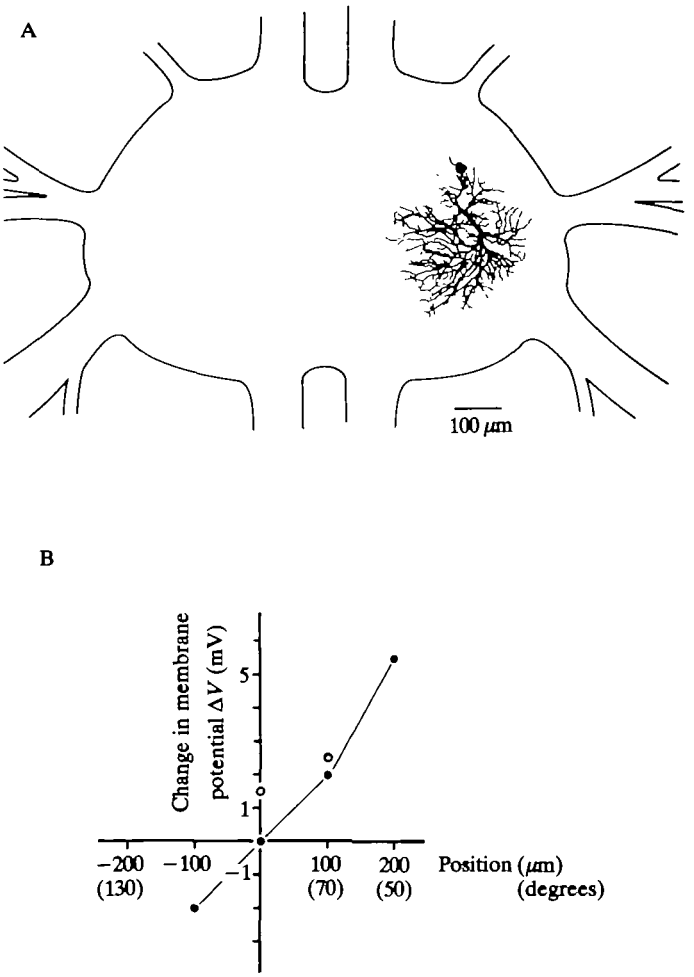

Fig. 12. Nonspiking interneurone of type E6. (A) Morphology; (B) plot of the change in membrane potential *versus* ChO position [from −100 μm to +200 μm (●) and back to 0 μm (○), always measured 4 s after the change of position].

Common characteristics of interneurones of types E1–E6

The membrane potentials of all the type E1–E6 interneurones were influenced by elongation movements at the ChO: they were all depolarized. Depolarization of these interneurones by current injection increased the activity of the spontaneously firing SETi motoneurone and also increased the SETi reflex activation induced by elongation stimuli at the ChO in all cases. Similar effects were shown by type E4 interneurones on FETi activity. Injecting hyperpolarizing currents into these interneurones never caused a failure of the resistance reflex in the SETi or FETi motoneurone, although in some cases there was a slight decrease of SETi activity. This implies that several processing pathways from the ChO to the extensor motoneurones act in parallel to produce the resistance reflex. An

example of the influence of individual interneurones on the resistance reflex in the extensor motoneurones was shown in detail for one type of E2 interneurone (see Fig. 4).

Nonspiking interneurones with inhibitory effects on the extensor motoneurones

Two types of nonspiking neurones were found which, when depolarized by current injection, decreased the spike frequency of SETi.

Type I1 (N=3)

The first type of interneurone was hyperpolarized by elongation stimuli (corresponding to joint flexion) and depolarized by relaxation stimuli. The morphology of an interneurone of this type is shown in Fig. 13A. The soma lay in the posterior part of the ganglion on a level with the posterior connectives. The primary neurite lay median in the ganglion. Most of the arborization occurred in a single plane of the ganglion.

Elongation stimuli (joint flexion) caused a marked hyperpolarization in this type of interneurone with a mean latency of 20.9±7.4 ms [N=9; velocity=±0.9 mm s^{-1} (approx. ±180 degrees s^{-1}); acceleration=147.9 mm s^{-2} (approx. ±2.9×10^4 degrees s^{-2})] for the interneurone shown in Fig. 13. Relaxation stimuli (joint extension) always caused a depolarization of this interneurone after a latency of 8.2±1.1 ms (N=9) (Fig. 13B). The amplitude of both responses increased with faster stimuli. There was a slight effect of ChO position on the membrane potential, the membrane potential being less negative when the ChO was in the relaxed position. Position effects were not investigated in more detail.

Depolarizing this interneurone by current injection caused a decrease in SETi activity, while hyperpolarizing it induced an increase of the spontaneous discharge rate of SETi (Fig. 13C). The activity of the FETi motoneurone was not obviously affected by tonically injected current without ChO stimulation. Tonically injecting current markedly altered the activity of the SETi motoneurone during the resistance reflex (Fig. 14). Hyperpolarization markedly increased the reflex activation of the SETi motoneurone and sometimes SETi spikes were detectable during relaxation stimuli at the ChO. Depolarizing currents markedly decreased the tonic activity of SETi and reduced the phasic stimulus response of the SETi motoneurone (Fig. 14). Depolarizing currents also seemed to reduce the number of FETi spikes during elongation of the ChO (Fig. 14).

This type of interneurone is involved in the generation of the resistance reflex in the extensor motoneurones by disinhibiting the SETi motoneurone during elongation stimuli (joint flexion). In addition, this interneurone is involved in the inhibition of the SETi motoneurone during and after relaxation movement (joint extension) of the ChO (see also Fig. 17, Ic).

Type I2 (N=2)

This type of interneurone was also depolarized during relaxation stimuli. The morphology of an interneurone of this type is shown in Fig. 15A. The soma lay

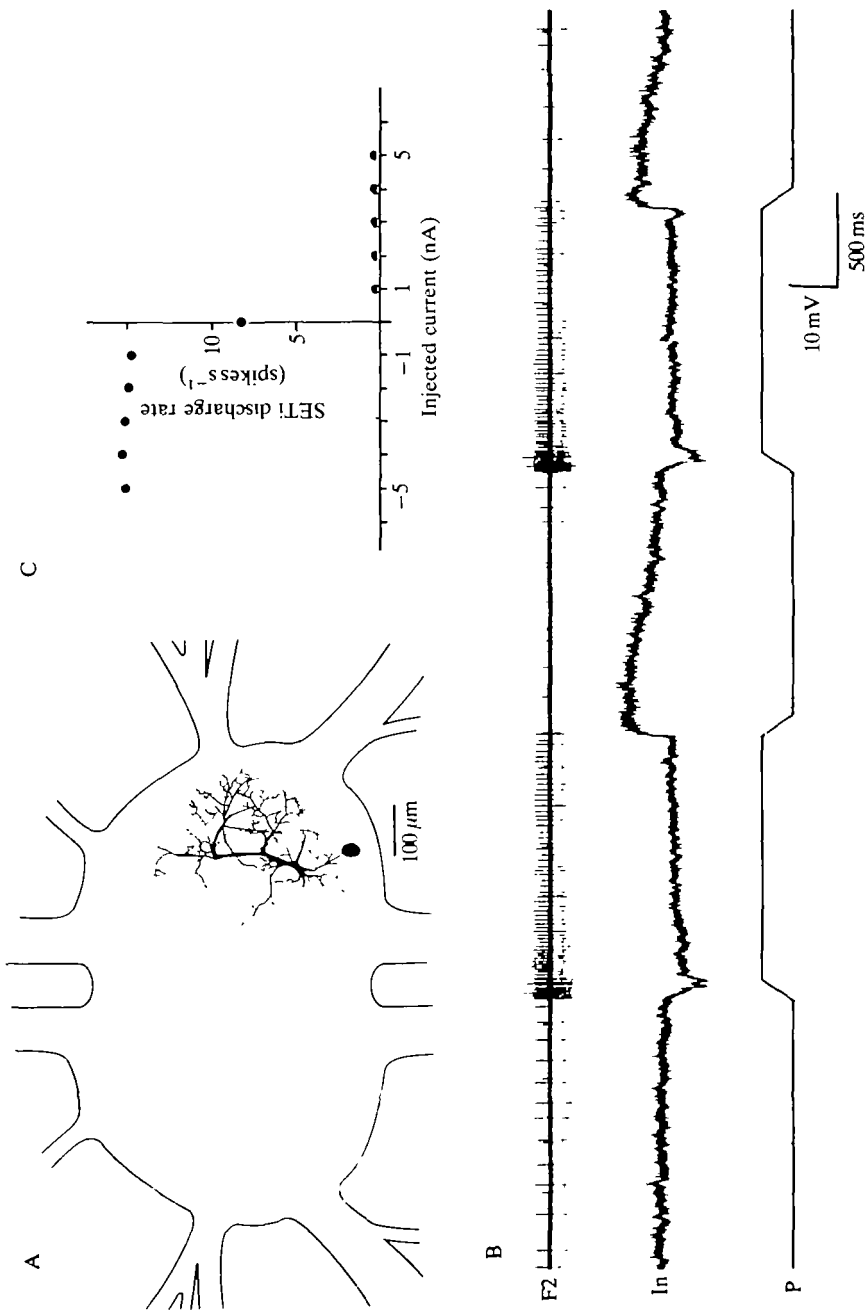

Fig. 13. Morphological and physiological properties of a nonspiking interneurone of type I1. (A) Morphology; (B) interneuronal response to trapezoidal stimulation of the ChO; (C) relationship between the current injected into the interneurone and the mean SETi discharge rate (from 4 to 12 s). F2, extensor nerve; In, interneurone; P, position.

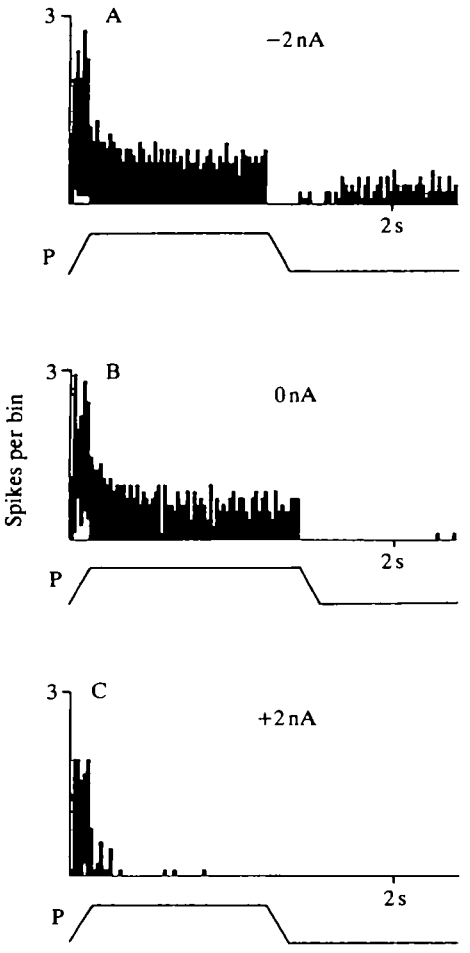

Fig. 14. Modulation of the resistance reflex in the SETi (black bars) and the FETi motoneurones (white bars) with different currents injected into the interneurone shown by peristimulus time histograms. (A,C) Average of 10 ramp-and-hold stimuli; (B) average of nine stimuli). P, position.

ipsilaterally in the posterior part of the ganglion at the level of the posterior connectives. Soma position and location of the primary neurite were similar to those of type I1, but the main arborizations were dorsally located and their shape was different from that of type I1 neurones.

The interneurones were depolarized by relaxation stimuli (joint extension) with a mean latency of 8.4±0.8 ms (N=9, velocity=+3.2 mm s^{-1}, acceleration=±489 mm s^{-2}). The amplitude of depolarization increased with increasing stimulus velocity. Elongation stimuli at the ChO induced a slight depolarization in the interneurone after a mean latency of 21.1±6.7 ms (N=9, velocity=−3.2 mm s^{-1}, acceleration=±489 mm s^{-2}) (Fig. 15B,C). Hyperpolarizing the interneurone with

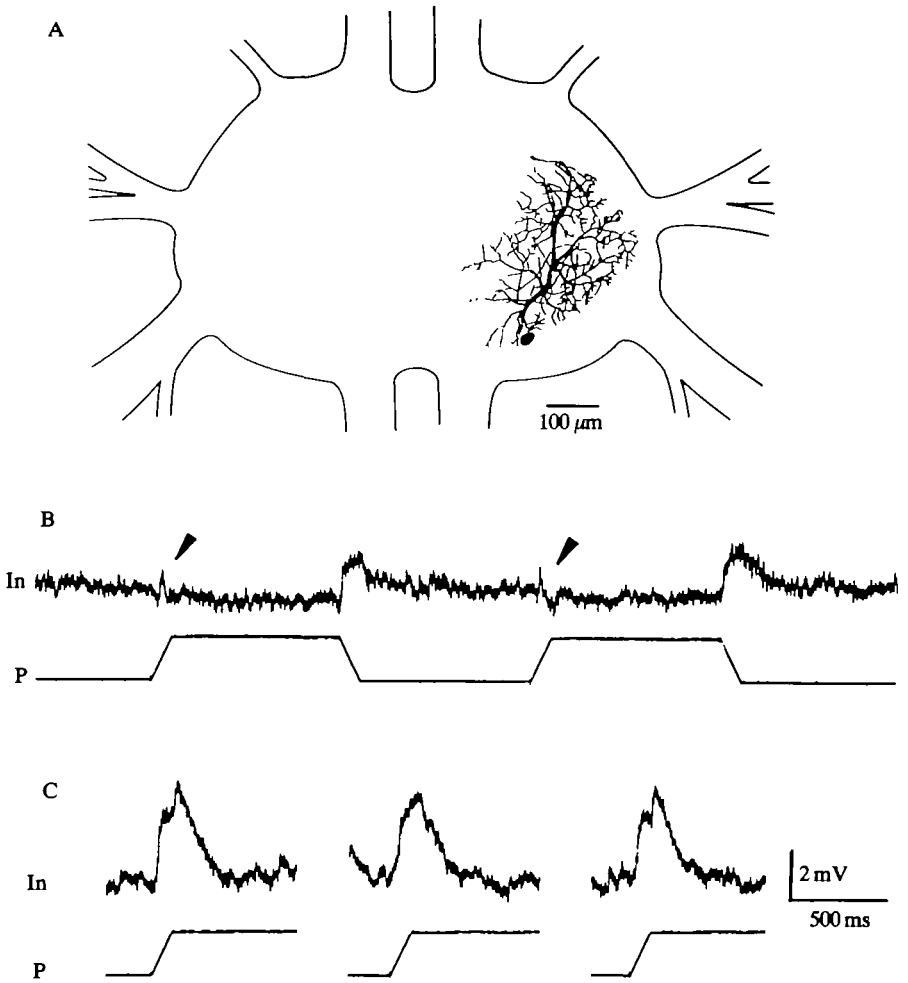

Fig. 15. Morphology and physiology of a nonspiking interneurone of type I2. (A) Morphology; (B) recording of the membrane potential during trapezoidal stimuli at the ChO; (C) depolarization of the interneurone during elongation ramps with hyperpolarized membrane potential. In, interneurone; P, position.

a small negative current (−1 nA) increased the amplitude of the depolarization during elongation ramps (Fig. 15C).

SETi activity depended on the membrane potential of this type of interneurone (tested by current injection) in a similar way as was shown for type I1 interneurones (see Fig. 13C). In all cases depolarization stopped SETi and FETi activity (Fig. 16), even in active animals.

The effects of current injections on the resistance reflex in the SETi motoneurone were the same as for type I1 interneurones, showing that type I2 interneurones influenced the activity of the extensor motoneurones in all the stimulus situations tested. This means that the type I2 interneurones are involved

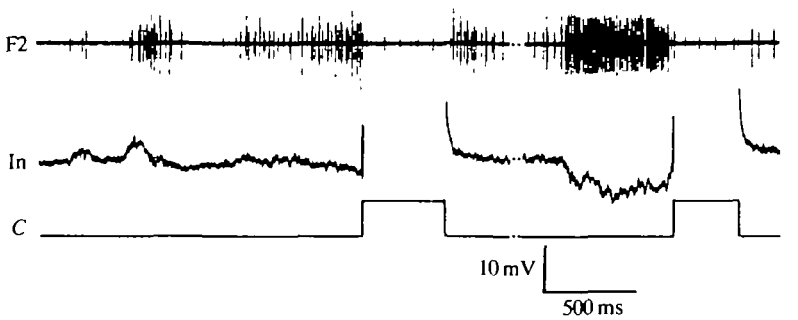

Fig. 16. Depolarization of nonspiking interneurones of type I1 or I2 abolishes spontaneous motor activity in the extensor nerve F2. F2 extensor nerve; In, interneurone; *C*, current.

in the generation of SETi inhibition during and after relaxation stimuli. As neurones of this type were slightly depolarized during elongation stimuli at the ChO, their physiology might be described as weakly opposing the generation of the resistance reflex in the extensor motoneurones (see Fig. 17, IIb).

Common characteristics of these interneurones

The membrane potential of these interneurones strongly influenced the activity of the SETi motoneurone. Injection of depolarizing currents caused a marked decrease of the phasic and tonic parts of the resistance reflex in the extensor motoneurones during elongation of the ChO (Fig. 14). Injection of hyperpolarizing currents caused a marked increase in SETi activity (Fig. 14). As these interneurones were depolarized during relaxation stimuli at the ChO, they contribute to the inhibition of SETi activity during relaxation of the ChO.

Discussion

Comparison with locusts

The present study reveals some morphological and physiological properties of nonspiking interneurones in the mesothoracic ganglion of the stick insect *Carausius morosus*. Local nonspiking interneurones have been most studied in the nervous system of the locust (Burrows, 1985, 1989; Siegler, 1985; Wilson and Phillips, 1983). A comparison of the morphology of nonspiking interneurones in the stick insect and in the locust shows that the type E4 interneurones in the stick insect have a very similar shape to one morphological type of interneurone found in the locust. These comparable interneurones have been described by Siegler and Burrows (1979) in the metathoracic ganglion and by Wilson (1981) in the mesothoracic ganglion of the locust. Wilson showed that the mesothoracic ganglion contained three interneurones of this type per half-ganglion, two of which drive flexor motoneurones while the third excites extensor motoneurones. On the basis of the gross morphology and of the output properties, the type E4

interneurones in the stick insect are very similar to the type DC VII2 interneurone (Wilson, 1981) in the locust mesothoracic ganglion. No comparable neurones could be found in the literature relating to locusts for the other nonspiking interneurones described in this paper.

Afferent signals from the ChO to the nonspiking interneurones

Excitation of the nonspiking interneurones of types E1–E6 during elongation and relaxation stimuli at the ChO was characterized by latencies of less than 8 ms (except type E2, where the latency was 10.1 ms) from the stimulus onset to the first intracellular response. The same was true for depolarization of neurones of types I1 and I2 during relaxation stimuli.

Current injection showed that in all these interneurones the depolarization induced by ChO signals was mediated chemically (as in Fig. 3C). The detailed structure of the connections from the ChO afferents to the nonspiking interneurones in the mesothoracic ganglion is unclear. In the locust it has been shown that the femoral chordotonal organ afferences make direct excitatory connections to flexor motoneurones, to spiking and to nonspiking interneurones (Burrows, 1987; Burrows *et al.* 1988).

In two cases interneuronal responses were measured after longer latencies: interneurones of types I1 and I2 during elongation stimuli. In both cases the interneurones were affected by ChO stimulation onset after about 20 ms; type I1 was hyperpolarized by IPSPs, type I2 was depolarized by EPSPs. This might be the effect of an information pathway from the ChO *via* intercalated interneurones to the recorded interneurone, as has been shown for inhibitory effects of ChO afferents on nonspiking interneurones in the locust (Burrows *et al.* 1988; Burrows, 1987).

The femur–tibia control loop contains resisting as well as assisting components

A general feature of the joint-control loops in the inactive stick insect is the generation of resistance reflexes in response to imposed movements. However, in the femur–tibia control loop Bässler *et al.* (1986) also found some minor 'assisting' components in the motor output. They showed that with fast relaxation stimuli at the ChO (joint extension) SETi and FETi are excited at the beginning of the relaxation stimulus, before they are hyperpolarized. They described the reverse sequence of responses for flexor motoneurones. These assisting components oppose the elicited resistance reflex in the femur–tibia joint, i.e. they assist an ongoing joint movement. They are small in amplitude so that the dominating resisting components in the control loop override them.

At the interneuronal level the same classification is useful to describe the different characteristics of the information pathways from the ChO to the motoneurones, such as those found in the present investigation. Resisting pathways are those that support the obvious motor output of the resistance reflex in the leg joint (e.g. an interneurone that is driving extensor motoneurones, when depolarized, is depolarized by signals from the ChO, signalling a joint flexion).

Assisting components are those that do not support the generation of the resistance reflex in the leg joint [when, for example, an interneurone is further depolarized by relaxation stimuli at the ChO (joint extension) and drives the SETi].

We were able to show for the different types of interneurones described in this paper (with the exception of type E1, where it was not tested), that they influenced the activity of SETi during elongation and relaxation displacements of the ChO. The structure of this connection (mono- or polysynaptic) is not known. Changes in the membrane potential of the interneurones were transmitted to the SETi motoneurone and, in the case of some interneurones, for example types E4 and I1, probably partly to the FETi motoneurone.

All neurones with excitatory effects on SETi were depolarized by an elongation stimulus. Since the elongation stimulus signals a joint flexion, they contribute to the generation of the resistance reflex in the SETi motoneurone and therefore form resisting pathways. The type I1 interneurones (with inhibitory effects on SETi) were hyperpolarized by an elongation of the ChO. As these interneurones disinhibit the SETi during elongation of the ChO, they are also part of the resisting pathways. For relaxation stimuli, neurones of types I1, I2 and to some extent E3 are part of a resisting pathway. In the locust, interneurones with comparable properties were described in the femur–tibia control loop of the hind leg (see Burrows *et al.* 1988) and in the pathways mediating local reflexes (Laurent and Burrows, 1988).

In contrast, interneurones of types E4, E5 and E6, which all had excitatory effects on SETi activity, were all depolarized during relaxation stimuli at the ChO. All these interneuronal pathways show assisting properties during relaxation stimuli at the ChO (see Fig. 17). At present we do not know if the depolarization of these interneurones during relaxation stimuli at the ChO (joint extension) is transmitted fully onto SETi. However, current injection showed that all these interneurones have an influence on SETi activity during relaxation stimuli at the ChO. When depolarizing current was injected into the interneurones during relaxation stimuli at the ChO, the SETi motoneurone was not totally inhibited (as in Fig. 11C,D). These assisting characteristics of the interneurones occurred in response to stimuli that elicited a resistance reflex in the extensor motoneurones. The stimuli can therefore be regarded as physiological, that is the feedback loop works properly. In addition, movement velocities up to 1800 degrees s^{-1} were found for active flexion movements in the femur–tibia joint of the stick insect (Bässler, 1983*a*), showing that the stimulus velocity values used should not be unphysiological for the femur–tibia joint.

The behavioural relevance of these pathways cannot be judged by the eliciting parameter values, as it is a main function of a joint–control loop in the inactive animal to resist imposed movements of the joint. Under natural conditions the joint–control loop has no influence on the parameter values of imposed movements.

In summary, there are two types of nonspiking interneuronal pathways: those

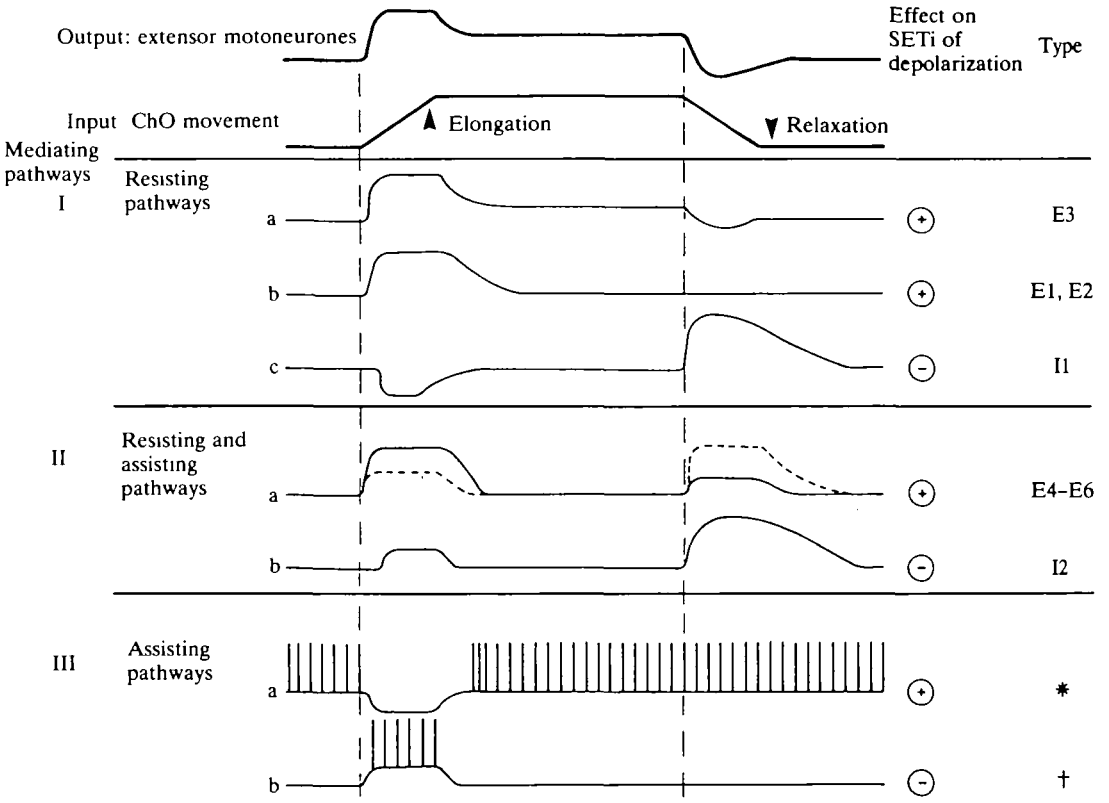

Fig. 17. Schematic time course of changes in the membrane potential of the different physiological types of interneurones (spiking and nonspiking) that transmit information in parallel from the ChO onto the SETi motoneurone. The types of mediating interneurones are grouped as: (I) resisting pathways, when they support the generation of any phase of the resistance reflex in the excitatory extensor motoneurones; (II) resisting and assisting pathways, when their physiology contains both supporting and opposing components in any phase of the resistance reflex in the excitatory extensor motoneurones; (III) assisting pathways, when their physiology only shows opposing characteristics on the generation of any phase of the resistance reflex in the extensor motoneurones (* Büschges, 1989*a*; † A. Büschges, unpublished results).

that contain only resisting components in the feedback loop (E1, E2, E3, I1) and those that contain resisting and assisting components (E4, E5, E6, I2). The results are summarized schematically in Fig. 17. In addition, two types of spiking local interneurones have been described showing only assisting components in the feedback loop (see Fig. 17 and Büschges, 1989*a*, Fig. 17). The properties of all these neurones indicate that the generation of a distinct resistance reflex is not only due to information processing that supports the detectable motor output (Fig. 10 in Burrows *et al.* 1988; Fig. 9 in Laurent and Burrows, 1988), but that supporting and opposing pathways are both involved in the production of the motor output. In other words, it seems likely that the output of the femur–tibia control loop

represents a sort of 'difference' between resisting and assisting components. The motor output itself also contains assisting components (Bässler *et al.* 1986) and the resulting movement represents the difference between resisting and assisting components.

Functional relevance of the resisting components in the femur–tibia control loop

The motor output of the femur–tibia control loop consists of two major stages during a resistance reflex, for both elongation (joint flexion) and relaxation (joint extension) movements of the ChO: (a) a phasic response of the motoneurones during position transients of the ChO (increase of SETi activity during elongation of the ChO; decrease of SETi activity during relaxation of the ChO) and (b) a tonic response during the subsequent static state of the ChO (Bässler, 1983*a*).

The interneurones of types E1–E6 and I1 are probably involved in the phasic increase of SETi discharge rate during elongation of the ChO (see the relationship between SETi activity and injected current for the different interneurones in addition to their stimulus response, and see the quantitative effects in a single interneurone shown in Figs 4 and 14). During relaxation of the ChO, interneurones of types I1, I2 and E3 support the decrease of SETi activity. Individual interneurones (for example, type E4 interneurones) process mainly velocity-dependent information during movement of the ChO. Thus, these pathways contribute to the velocity sensitivity of the whole system (see Bässler, 1983*a*, 1988).

Tonic increase or decrease of the SETi discharge rate by ChO positioning is supported by the physiology of interneurones of types E3 and E6. Elongated ChO positions induce a more depolarized membrane potential in the nonspiking interneurones that drive the SETi motoneurone.

Analysis of the role of single interneurones during the generation of the resistance reflex in the extensor motoneurones showed that the control loop consists of parallel pathways transmitting information from the ChO onto the extensor motoneurones. This is especially true for the interneurones involved in the generation of the resistance reflex during elongation movements of the ChO. Hyperpolarization of any interneurone never led to the failure of the resistance reflex in the extensor motoneurones. However, this rather qualitative statement does not imply that the information pathways in the control loop are parallel or equal in their quantitative contribution to the total effect in the control loop.

This work was supported by a grant from the Deutsche Forschungsgemeinschaft (Ba 578) to U. Bässler. I gratefully acknowledge the constant interest and support given to me by Professor Ulrich Bässler. Professor Fred Delcomyn and Drs Rolf Kittmann, Uwe Koch and Josef Schmitz read this paper in manuscript, and I greatly appreciate their helpful comments. I also thank Professor Malcolm Burrows for his advice on recording from nonspiking neurones. Finally, my thanks are due to I. Winkler-Reske for help with some of the figures and S. Watt for typing the manuscript.

References

BÄSSLER, U. (1977). Sense organs in the femur of the stick insect and their relevance to the control of the position of the femur–tibia joint. *J. comp. Physiol.* **121**, 99–113.

BÄSSLER, U. (1983*a*). *Neural Basis of Elementary Behavior in Stick Insects*. Berlin, Heidelberg, New York: Springer Verlag.

BÄSSLER, U. (1983*b*). The neural basis of catalepsy in the stick insect *Cuniculina impigra*. III. Characteristics of the extensor motor neurons. *Biol. Cybernetics* **46**, 159–165.

BÄSSLER, U. (1988). Functional principles of pattern generation for walking movements of stick insect forelegs: the role of the femoral chordotonal organ afferences. *J. exp. Biol.* **136**, 125–147.

BÄSSLER, U., HOFMANN, T. AND SCHUCH, U. (1986). Assisting components within a resistance reflex of the stick insect, *Cuniculina impigra*. *Physiol. Ent.* **11**, 359–366.

BURROWS, M. (1981). Local interneurones in insects. In *Neurones Without Impulses* (ed. A. Roberts and B. M. H. Bush), pp. 199–221. Cambridge: Cambridge University Press.

BURROWS, M. (1985). Nonspiking and spiking local interneurons in the locust. In *Model Neural Network and Behavior* (ed. A. I. Selverston), pp. 109–125. New York and London: Plenum Publishing Corporation.

BURROWS, M. (1987). Inhibitory interactions between spiking and nonspiking local interneurons in the locust. *J. Neurosci.* **7**, 3282–3292.

BURROWS, M. (1989). Processing of mechanosensory signals in local reflex pathways of the locust. *J. exp. Biol.* **146**, 209–227.

BURROWS, M., LAURENT, G. J. AND FIELD, L. H. (1988). Proprioceptive inputs to nonspiking local interneurons contribute to local reflexes of a locust hindleg. *J. Neurosci.* **8**, 3085–3093.

BÜSCHGES, A. (1989*a*). Processing of sensory input from the femoral chordotonal organ by spiking interneurones of stick insects. *J. exp. Biol.* **144**, 81–111.

BÜSCHGES, A. (1989*b*). Nonspiking interneurones in the femur–tibia joint controlling feedback loop in the stick insect *Carausius morosus*: The change of neurone response as a function of the behavioural state. In *Dynamics and Plasticity in Neuronal Systems. Proceedings of the 17th Göttingen Neurobiology Conference* (ed. N. Elsner and W. Singer), p. 230. Stuttgart, New York: Georg Thieme Verlag.

DEBRODT, B. AND BÄSSLER, U. (1989). Motor neurones of the flexor muscle in phasmids. *Zool. Jb. Physiol.* **93**, 481–494.

DEBRODT, B. AND BÄSSLER, U. (1990). Responses of flexor motoneurones to stimulation of the femoral chordotonal organ of the phasmid *Extatosoma tiaratum*. *Zool. Jb. Physiol.* (in press).

HENGSTENBERG, R. (1977). Spike responses of 'non-spiking' visual interneurone. *Nature, Lond.* **270**, 338–340.

HOFMANN, T. AND KOCH, U. T. (1985). Acceleration receptors in the femoral chordotonal organ in the stick insect, *Cuniculina impigra*. *J. exp. Biol.* **114**, 225–237.

HOFMANN, T., KOCH, U. T. AND BÄSSLER, U. (1985). Physiology of the femoral chordotonal organ in the stick insect, *Cuniculina impigra*. *J. exp. Biol.* **114**, 207–223.

KITTMANN, R. (1984). Quantitative Analyse von Verstärkungsänderungen eines Gelenkstellungsregelkreises. Dissertation, Universität Kaiserslautern.

LAURENT, G. J. AND BURROWS, M. (1988). Direct excitation of nonspiking local interneurones by exteroceptors underlies tactile reflexes in the locust. *J. comp. Physiol.* **162**, 563–572.

RUPPEL, A. (1988). Vier Programme zur Meßdatenerfassung und Meßdatenspeicherung mit dem IBM Data Aquisition and Control Adaptor. Projektarbeit, Fachbereich Informatik, Universität Kaiserslautern, Teil I,II.

SCHMITZ, J., BÜSCHGES, A. AND DELCOMYN, F. (1988). An improved electrode design for en passant recording from small nerves. *Comp. Biochem. Physiol.* **91A**, 769–772.

SIEGLER, M. V. S. (1985). Nonspiking interneurons and motor control in insects. *Adv. Insect Physiol.* **18**, 249–304.

SIEGLER, M. V. S. AND BURROWS, M. (1979). The morphology of local non-spiking interneurones in the metathoracic ganglion of the locust. *J. comp. Neurol.* **183**, 121–148.

WATKINS, B. L., BURROWS, M. AND SIEGLER, M. V. S. (1985). The structure of locust nonspiking interneurones in relation to the anatomy of their segmental ganglion. *J. comp. Neurol.* **240**, 233–255.

WEIDLER, D. J. AND DIECKE, F. P. J. (1969). The role of cations conduction in the central nervous system of the herbivorous insect *Carausius morosus*. *Z. vergl. Physiol.* **64**, 372–399.

WEILAND, G., BÄSSLER, U. AND BRUNNER, M. (1986). A biological feedback system with electronic input: the artificially closed femur–tibia control system of stick insects. *J. exp. Biol.* **120**, 369–385.

WILSON, J. A. (1981). Unique, identifiable local nonspiking interneurons in the locust mesothoracic ganglion. *J. Neurobiol.* **12**, 353–366.

WILSON, J. A. AND PHILLIPS, C. E. (1983). Pre-motor non-spiking interneurons. *Prog. Neurobiol.* **20**, 89–107.

ZARNACK, W. AND MÖHL, B. (1976). A data acquisition processor with data reduction for electrophysiological experiments. *Fortschr. Zool.* **24**, 321–326.